
Volume 229, 25 August, 2013
ISSN 0257-8972
ELSEVIER
SURFACE & COATINGS TECHNOLOGY
The Eleventh International Workshop on
Plasma-Based Ion Implantation and Deposition
8–12 September 2011, Harbin, China
Editors
S. Aouadi
H.C. Man
P.J. Martin
A. Matthews
J. Patscheider
I. Petrov
Proceedings Editors
K. Yukimura
P.K. Chu
X. Ma
X. Tian
Available online at www.sciencedirect.com
SciVerse ScienceDirect
http://www.elsevier.com/locate/surfcoat

Surface & Coatings Technology 229 (2013) 105–108

Contents lists available at SciVerse ScienceDirect

Surface & Coatings Technology

journal homepage: www.elsevier.com/locate/surfcoat

High-temperature stability of $TiAlN/TiB_2$ multilayers grown on Al_2O_3 substrates using IBAD

J.Y. Yan [a], Y.D. Sun [a], D.J. Li [a,*], M.Y. Liu [a], L. Dong [a], M. Cao [a], C.K. Gao [a], N. Wang [a], X.Y. Deng [a], H.Q. Gu [b,c], R.X. Wan [b,c], X. Sun [d]

[a] College of Physics and Electronic Information Science, Tianjin Normal University, Tianjin 300387, China
[b] Tianjin Institute of Urological Surgery, Tianjin Medical University, Tianjin 300070, China
[c] Ninth People's Hospital, Shanghai Jiao Tong University, School of Medicine, Shanghai 200011, China
[d] Department of Mechanical & Materials Engineering, University of Western Ontario, London, ON, Canada

ARTICLE INFO

Available online 27 January 2013

Keywords:
$TiAlN/TiB_2$ multilayers
Ion beam assisted deposition
Thermal stability
Annealing
Hardness

ABSTRACT

$TiAlN/TiB_2$ multilayers which have various modulation ratios (t_{TiAlN}:t_{TiB2}) ranging from 1:6 to 18:1 were synthesized on Al_2O_3(111) substrate by ion beam assistant deposition (IBAD). The effects of annealing on the mechanical and structural properties of the multilayers were investigated using X-ray diffractometry (XRD), scanning electron microscope (SEM), transmission electron microscope (TEM), and Nanoindenter (CSM instruments). It was found that the hardness for all multilayers was higher than TiAlN or TiB_2 monolayer and the highest hardness of 43 GPa was attained at t_{TiAlN}:t_{TiB2} = 16:1. The multilayers show the polycrystallines of TiAlN(111) and (220) textures. The thermal stability characteristics of the multilayers were studied in vacuum furnace for 30 min at temperatures of 500 and 700 °C. Compared with as-deposited multilayers, the annealed multilayers displayed a stable hardness and elastic modulus and an increased fracture resistance. It was found that the multilayers showed good thermal stability.

1. Introduction

With the development of science and technology, it has been highly demanded in the cutting industry to improve the efficiency and the accuracy of the process both in high speed machining and in lubricant free dry cutting.

Since TiAlN was considered as an excellent coating material due to its high hardness, wear and oxidation resistance [1,2], the incorporation of other materials and the control of microstructure have been investigated to further improve its mechanical properties. As an incorporation material, TiB_2 was chosen for the present investigation, because it has widespread application in cutting tools or machine parts due to its high hardness, wear resistance, chemical inertness and high-temperature stability [3–6]. There have been increasing interests in fabrication of this material in thin films and coatings for many potential applications, for example, to reduce wear and corrosion in engineering components and particularly in material processing tools [7–11]. For the TiAlN based on nano-structured coatings, thermal stability as well as hardness and wear resistance was reported to be much superior to those of TiAlN coating [12], as reported in (Ti,Cr,Al)N/(Al,Si)N multilayers [13]. TiB_2 monolayer and TiAlN monolayer both have high hardness and high-temperature stability, therefore, $TiAlN/TiB_2$ multilayers might display superior mechanical properties and thermal stability in suitable conditions and structure.

In previous works [14,15], the research about as-deposited $TiAlN/TiB_2$ multilayers with different modulation periods ranging from 0.6 to 27 nm and modulation ratios ranging from 8:1 to 25:1 were deposited on Si(100) substrate and proved that as-deposited $TiAlN/TiB_2$ multilayers have better mechanical properties in a small modulation period [14]. In order to investigate the high temperature stability of this system, we further studied the influence of annealing on its structure and properties [15]. Despite better thermal stability and over 40 GPa hardness displayed on a $TiAlN/TiB_2$ multilayer grown on a Si(100) substrate at t_{TiB2}:t_{TiAlN} = 1:14 under the condition of annealing of 500 °C, there occurred serious delamination in annealed multilayers when annealing temperature exceeded 500 °C. The main reason could be a big difference in stress and hardness between the annealed multilayer and Si(100) substrate at high temperature. It is well known, that high temperature stability of the coatings is a key concern since new environment regulations are requiring the removal of coolants and lubricants from the cutting process. So, multilayers have to be exposed to elevated temperatures during high-speed cutting or dry cutting process. Therefore, producing multilayers with a good thermal stability at 700–1000 °C, and hence keeping better mechanical and tribological behaviors becomes crucial.

* Corresponding author at: 393#, Mingli Building, Bin Shui Xi Road, Xiqing District, Tianjin, China. Tel./fax: +86 22 23766519.
E-mail address: dejunli@mail.tjnu.edu.cn (D.J. Li).

0257-8972/$ – see front matter © 2013 Elsevier B.V. All rights reserved.
http://dx.doi.org/10.1016/j.surfcoat.2012.12.051

In order to further enhance the thermal stability of this multilayered system at higher annealing temperature, in this work, we chose $Al_2O_3(111)$ to replace Si(001) as substrate to support 700 °C or higher temperature treatment of TiAlN/TiB_2 multilayers due to the excellent high temperature stability and high hardness of Al_2O_3. The thermal stability in the structure and mechanical properties was evaluated by annealing in vacuum at temperatures of 500 to 700 °C. Our aim is to explore how structural stability affected the mechanical properties during high-temperature treatment.

2. Experimental details

An IBAD system (FJL560CI2, Chinese Academy of Science) was used to synthesize TiAlN/TiB_2 multilayers on $Al_2O_3(111)$ substrates. An IBAD system with two ion sources, one rotatable water-cooled sample holder, and one rotatable water-cooled target holder with four sides was used to synthesize TiAlN, TiB_2, and TiAlN/TiB_2 multilayers. First of all, the substrates were cleaned in an ultrasonic agitator in acetone and alcohol for at least 15 min and dried using compressed air after each cleaning cycle. A second cleaning process was done on the IBAD system where the substrates were sputter-cleaned at vacuum for 5 min by Ar^+ (500 eV, 5 mA) bombardment. The introduction of Ar and N_2 gas to the two ion sources were independently controlled using the mass-flow controllers. In order to enhance the adhesion between the multilayer and the substrate, a 40 nm-thick Ti buffer layer was deposited on substrates by Ar^+ beam sputtering Ti target (99.95% purity) and then TiAlN and TiB_2 layers were deposited alternately. The TiB_2 and TiAl targets (both 99.95% purity) were sputtered alternately by Ar^+ beam (1.05 keV, 25 mA) to deposit on the substrates and the resulting coatings were simultaneously bombarded with N^+ (250 eV, 5 mA). Meanwhile, there was a shutter in front of N^+ bombardment to block the influence of the TiB_2 layer. The shutter has kept pace with a computer program. The base pressure of the vacuum chamber was 2.0×10^{-4} Pa. The deposition was carried out at a pressure of 1.3×10^{-2} Pa. A series of TiAlN/TiB_2 multilayers with a constant modulation period (bilayer thickness, Λ) and different modulation ratio (the thickness ratio of TiAlN and TiB_2 layers at a constant Λ, t_{TiAlN}:t_{TiB2}) ranging from 18:1 to 1:6 were prepared. All multilayers were grown to a thickness of about 450 nm. In order to measure the thermal stability, TiAlN/TiB_2 multilayers were heated in vacuum at a pressure of 2.0×10^{-4} Pa. The purpose is to hope to fix the multilayer's structure by annealing in vacuum before the real cutting process in air. Annealing involved increasing the temperature of the samples from room temperature to the desired temperature (500 and 700 °C) at a slow heating rate of 2 °C/min and maintaining the desired temperature for 30 min. Subsequently, the samples were cooled down at a rate of 2 °C/min.

The cross-section image of the multilayers was observed by field-emission scanning electron microscopy (SEM, Hitachi 4800, Japan). The nano-structure was investigated with a JEM 2100 transmission electron microscope (TEM). A D/MAX 2500 diffractometer used for crystallinity analysis was operated with Cu Kα radiation at 1.54056 Å. The formation of the nanoscale layered structure was confirmed by X-ray reflectivity (XRR) data [16]. The hardness and elastic modulus of the multilayers as a continuous function of depth from a single indentation were obtained by the continuous stiffness measurement (CSM) technique using a Nano Indenter XP system that employed a Berkovich diamond indenter. Fifteen hardness measurements have been made for each sample. This system was also used to perform scratch test. In this test, the maximum load was up to 100 mN on multilayers, and the maximum load was 120 mN on annealed multilayers in order to measure fracture resistance.

3. Results and discussion

Firstly, we designed a type of TiAlN/TiB_2 multilayer with an estimated Λ of 8 nm and a t_{TiAlN}:t_{TiB2} of 1:1 according to real deposition rates of TiAlN and TiB_2 layers. To prove the estimated Λ or t_{TiAlN}:t_{TiB2} values and deposition rate coherence, we employed SEM, TEM, and XRR. According to this design process, we prepared a series of TiAlN/TiB_2 multilayers at a constant Λ and different t_{TiAlN}:t_{TiB2} to study the effects of t_{TiAlN}:t_{TiB2} and annealing on the mechanical and structural properties. Fig. 1(a) provides cross-sectional SEM and TEM images of this TiAlN/TiB_2 multilayer. The SEM image gives direct information on the existence of a well-defined composition modulation and layered structure in the multilayer. In this SEM image, Λ is observed to be about 8 nm. The light and dark colored layers, TiB_2 and TiAlN layers, are almost equal in width, which means that the thickness ratio of TiAlN and TiB_2 layers within 8 nm-thick Λ, i.e. modulation ratio (t_{TiAlN}:t_{TiB2}), is 1:1. The nanoscale multilayered structure is clearly observed in the SEM image. This is direct evidence of about 8 nm-thick Λ and t_{TiAlN}:t_{TiB2} = 1:1 which is close to our design value according to the deposition rate of TiAlN and TiB_2 layers. The TEM image in this figure shows the existence of TiAlN(111) crystallinity, implying that TiAlN phases are embedded in the amorphous structure of TiB_2. For TiAlN/TiB_2 multilayers at higher t_{TiAlN}:t_{TiB2}, we believe that dominant nanocrystalline TiAlN are embedded in amorphous TiB_2 phases, because TiAlN is a thick layer within every modulation period and showed the polycrystalline in the multilayers. The dominant nanocrystalline TiAlN surrounded by amorphous phases can produce a positive effect on the mechanical strength of the multilayers [17].

Clear reflection peaks are observed in XRR patterns (Fig. 1(b)) of a TiAlN/TiB_2 multilayer, indicating the existence of relatively sharp and flat interfaces and distinct layer structures in this multilayer again. In this figure, the lattice fringe clearly shows that TiB_2 and TiAlN layers form a superlattice. Sharp interfaces between the two layers throughout the whole multilayer can cause an enhancement in hardness. This 8 nm-thick Λ is also proved by the calculated value from the XRR

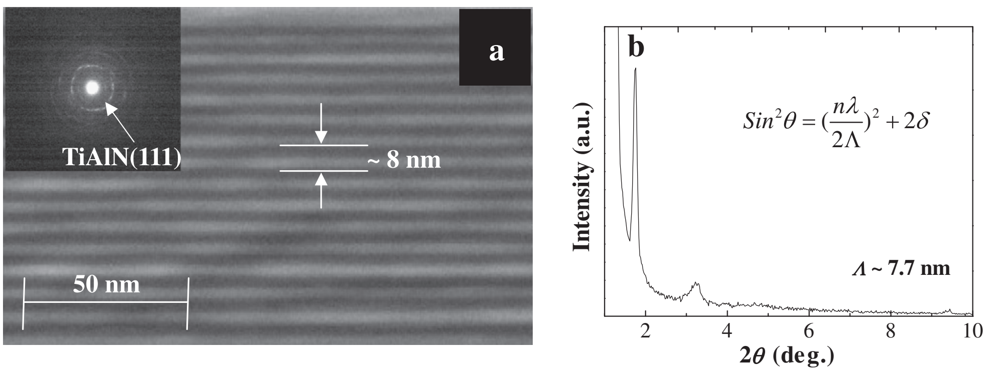

Fig. 1. (a) SEM and TEM images and (b) XRR patterns of TiAlN/TiB_2 multilayer at estimated Λ = 8 nm.

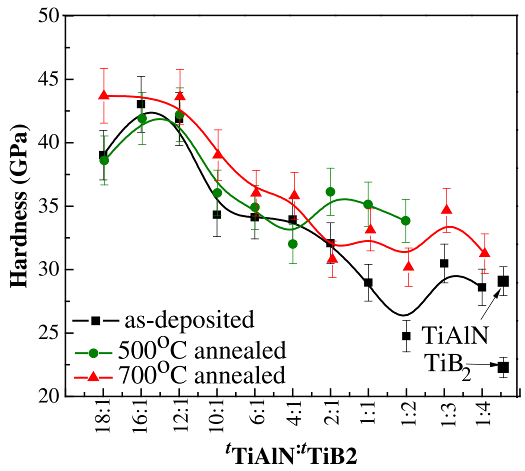

Fig. 2. Hardness of TiAlN/TiB_2 multilayers *vs.* t_{TiAlN}:t_{TiB2} before and after annealing at 500 °C and 700 °C.

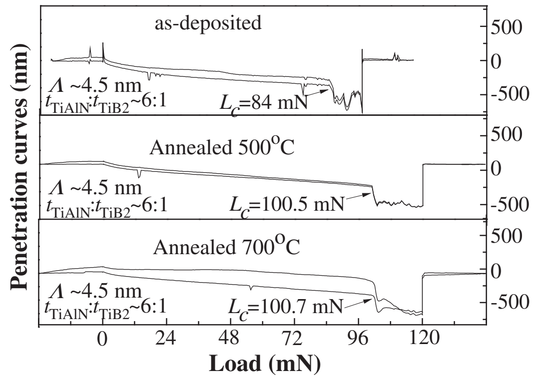

Fig. 4. Surface profiles of the scratch-scan on multilayers before and after annealing 500 °C and 700 °C.

result in Fig. 1(b). The Λ value is calculated to be about 7.7 nm according to the periodic positions of the reflection peaks using the modified Bragg's law [18,19], given by $\mathrm{Sin}^2\theta = \left(\frac{n\lambda}{2\Lambda}\right)^2 + 2\delta$, where Λ is the modulation period, n is the integer reflection order number, $\lambda = 1.54056$ Å and δ related to the average reflective index n. As it is expected from the equation above, all the data points fit very well on a straight line, from which Λ is determined. The detailed method can be seen in our previous work [20]. The Λ of 7.7 nm is in agreement with the 8 nm value of SEM observation. Therefore, it also proves the actual result according to experimental design.

Based on our previous works about TiAlN/TiB_2 multilayers [15], a modulation period of 4.5 nm has better mechanical and structural properties. In our published article [15], a clean cross-sectional SEM image of a 4.5 nm-thick Λ multilayer has been provided. So, in order to develop this system at a temperature of 700 °C or higher, a series of TiAlN/TiB_2 multilayers at a constant Λ of 4.5 nm and different t_{TiAlN}:t_{TiB2} are prepared. Fig. 2 shows the hardness of as-deposited and annealed multilayers with different t_{TiAlN}:t_{TiB2}, together with the hardness of TiAlN and TiB_2 monolayers. For all the as-deposited multilayers, the hardness is higher than that of the TiAlN monolayer. With increasing t_{TiAlN}:t_{TiB2}, the hardness of multilayers tends gradually to reach a maximum (43 GPa) and then decreases. In our other work about TiAlN/TiB_2 multilayers synthesized by magnetron sputtering [21], the TiAlN/TiB_2 multilayers with modulation ratios ranging from 1:4 to 1:1 have similar change and displayed the highest hardness (36 GPa) at t_{TiAlN}:t_{TiB2} = 2:5. Compared with that work, higher hardness appears at higher t_{TiAlN}:t_{TiB2} in this work. The maximum hardness of about 43 GPa is reached at t_{TiAlN}:t_{TiB2} = 16:1. We believe that the periodic insertion of thinner amorphous TiB_2 into TiAlN induces TiAlN(111) and (220) texture growth, contributing to hardness increasing.

For the application of nano-structured coating with two phases (nanoscale multilayered and nanocomposite coatings) at high temperatures, thermal stability should be considered because intermixing can occur between the two phases by interdiffusion, which causes degradation of mechanical properties of the multilayers at high temperatures [22,23]. For our TiAlN/TiB_2 multilayers, no significant change in hardness at higher t_{TiAlN}:t_{TiB2} from 4:1 to 18:1 is observed before and after annealing at 500 and 700 °C. The maximum hardness of about 43 GPa is reached at t_{TiAlN}:t_{TiB2} = 16:1–18:1 after annealing. Whereas annealed multilayers at lower t_{TiAlN}:t_{TiB2} from 1:4 to 2:1 display a slight enhancement in hardness. This thermal stability in hardness is related to the thermal stability in layered and polycrystalline structure.

Fig. 3 reveals the elastic modulus of TiAlN and TiB_2 monolayers as well as-deposited and annealed multilayers with different t_{TiAlN}:t_{TiB2}. The elastic modulus strongly depend on t_{TiAlN}:t_{TiB2}. Compared to be invariable between t_{TiAlN}:t_{TiB2} = 8:1 and t_{TiAlN}:t_{TiB2} = 18:1, the elastic modulus of t_{TiAlN}:t_{TiB2} ranging from t_{TiAlN}:t_{TiB2} = 1:4 to t_{TiAlN}:t_{TiB2} = 8:1 increased in a certain extent before and after annealing (500 and 700 °C). Its change trend is similar with that of hardness.

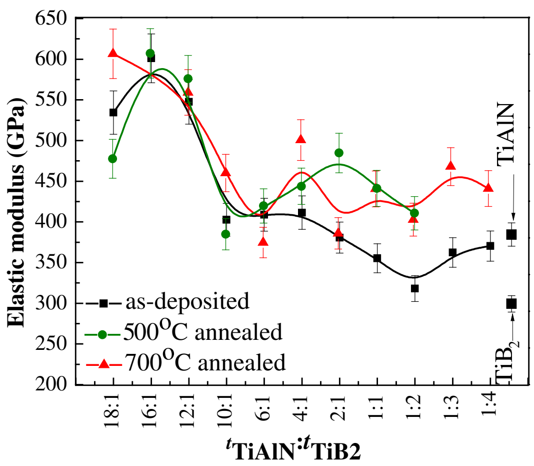

Fig. 3. Elastic modulus of TiAlN/TiB_2 multilayers *vs.* t_{TiAlN}:t_{TiB2} before and after annealing 500 °C and 700 °C.

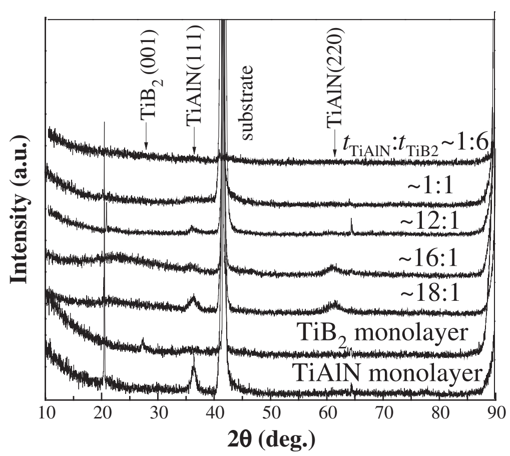

Fig. 5. XRD patterns of as-deposited TiAlN/TiB_2 multilayers with different t_{TiAlN}:t_{TiB2}.

Interfaces act as barriers to the motion of dislocations in multilayers. In addition, as the layer thickness and crystallite size approach nanometer dimensions, dislocation nucleation becomes energetically unfavorable. Both factors make multilayers stronger than expected from the rule of mixtures [24]. On the other hand, according to Koehler's theory, materials in lamellar structure with different shear moduli also show hardness enhancement. For TiAlN/TiB_2 multilayers, the shear moduli of both materials can be calculated by $G = E/2(1 + \nu)$, where G is the shear modulus, E is the Young's modulus and ν (0.25) is the Poisson ratio. The calculated G_{TiAlN} and G_{TiB2} are 133.3 GPa and 67.0 GPa, respectively. The difference in shear moduli of the two materials is very large, which means that there is a great contribution in the hardening mechanism by Koehler's theory.

We all know that high hardness of coatings is related to its high residual stress, which is the main reason for coating delamination and plastic deformation. Therefore, the relative lower residual stress and higher hardness in coatings is a key factor for these coatings to explore more applications. In this work, delamination occurs at the hardest multilayer at t_{TiAlN}:t_{TiB2} = 16:1 after annealing of 700 °C at the start of scratch processing. So the scratch test is hard to be performed for the hardest multilayer at 700 °C. The main reason is due to its superhardness (over 43 GPa) inducing a big difference in stress between multilayer and substrate, which leads to the delamination of the multilayer. Therefore, we choose multilayer with higher hardness (36 GPa) at t_{TiAlN}:t_{TiB2} = 6:1 to perform the scratch test. Fig. 4 shows the surface profiles of the scratch-scans made on the multilayer at Λ = 4.5 nm and t_{TiAlN}:t_{TiB2} = 6:1 before and after annealing at 500 and 700 °C. The critical load (*Lc*) of scratch associated with the abrupt change in the scratch-scan profile is related to the fracture resistance of the multilayers. As-deposited multilayer indicates a maximum *Lc* of 84 mN. The clear surface profiles of the scratch-scans after annealing at 500 and 700 °C are shown in this figure. Their *Lc* values are over 100 mN, displaying the higher indentation fracture resistance. The increased fracture resistance may be interrelated with the releasing of internal stress and increasing of plastic recovery of the multilayers with layered structures after annealing.

XRD patterns of as-deposited multilayers with different t_{TiAlN}:t_{TiB2} at a constant modulation period of 4.5 nm and a monolayer of TiAlN and TiB_2 are shown in Fig. 5. TiAlN layer shows a strong (111) peak, while TiB_2 is observed as a weak (001) peak in monolayer coatings. To TiAlN/TiB_2 multilayers, this weak TiB_2 (001) peak disappears, displaying the main amorphous structure in TiB_2 layers of TiAlN/TiB2 multilayers [14,15,25]. With increasing t_{TiAlN}:t_{TiB2}, the polycrystalline of TiAlN(111) and (220) becomes stronger, indicating better crystallinity. This structure change is ascribed to grains growth induced by amorphous TiB_2 periodic insertion. The combined nanocrystallities and amorphous phases can produce a positive effect on mechanical properties.

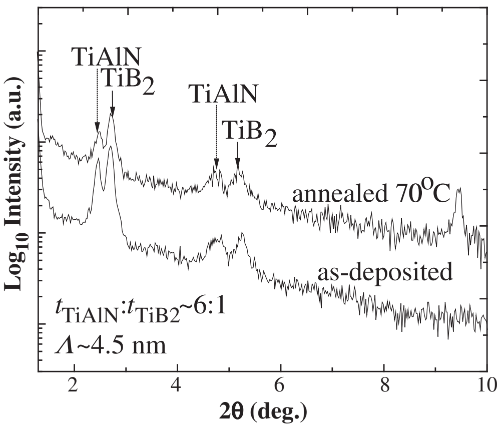

Fig. 6. High resolution XRR patterns of as-deposited and 700 °C annealed TiAlN/TiB_2 multilayers at Λ = 4.5 nm.

In order to investigate and compare detailed interfacial information of the multilayer at Λ = 4.5 nm before and after annealing at 700 °C, the high resolution XRR curve is given in Fig. 6 by taking the base 10 logarithm of the intensity values. The clear Kiessig fringes appeared in this figure still prove the alternating appearance of TiAlN and TiB_2 individual layers in its structure. No visible change in XRR peak position and intensity is observed before and after annealing, which means a good thermal stability in the layered structure of the multilayer.

4. Conclusion

In this work, Al_2O_3(111) was employed as substrate to grow TiAlN/TiB_2 multilayers. Our purpose was to gain insight into the thermal stability of TiAlN/TiB_2 multilayers. The thermal stability in hardness, elastic modulus and structure of TiAlN/TiB_2 multilayers prepared by alternating deposition of TiAl and TiB_2 targets was investigated. By carefully controlling modulation ratios to lower values, IBAD can produce a TiAlN/TiB_2 multilayer with the highest hardness of 43 GPa at t_{TiAlN}:t_{TiB2} = 16:1. The highest critical load of over 100 mN was attained after annealing at 700 °C, implying the improved fracture resistance. The stable layered structure and the strengthened TiAlN(111) and (220) textures after annealing were the main reasons for the thermal stability in hardness and the increased fracture resistance at high temperature.

Acknowledgements

This work was supported by the National Basic Research Program of China (973 Program, 2012CB933600), the National Natural Science Foundation of China (51272176 and 11075116).

References

[1] A. Hörling, L. Hultman, M. Odén, J. Sjölén, L. Karlsson, Surf. Coat. Technol. 191 (2005) 384.
[2] K. Chu, Y.G. Shen, W.-D. Münz, J. Vac. Sci. Technol. A 21 (1986) 2717.
[3] W. Herr, B. Matthes, E. Broszeit, K.H. Kloos, Mater. Sci. Eng., A 140 (1991) 616.
[4] L. Dong, G.Q. Liu, Y.D. Sun, M.Y. Liu, D.J. Li, Int. J. Mod. Phys. B 24 (2010) 43.
[5] T. Shikama, Y. Sakai, M. Fukutomi, M. Okada, Thin Solid Films 156 (2) (1988) 287.
[6] S. Shimada, M. Takahashi, H. Kiyono, J. Tsujino, Thin Solid Films 516 (2008) 6616.
[7] X. Chu, S.A. Barnett, Appl. Phys. 77 (1995) 4403.
[8] J. Chen, J.A. Barnard, Mater. Sci. Eng. A 191 (1995) 233.
[9] E. Matsubara, Y. Waseda, S. Takeda, Y. Taga, Thin Solid Films 86 (1990) L133.
[10] R. Wiedemann, R. Oettel, M. Jerenz, Surf. Coat. Technol. 97 (1997) 313.
[11] B. Todorović, T. Jokić, Z. Rakočević, Z. Marković, B. Gaković, T. Nenadović, Thin Solid Films 300 (1997) 272.
[12] M. Cao, L. Dong, G.Q. Liu, D.J. Li, Nanoeng. Nanosyst. 223 (2009) 23.
[13] N. Fukmoto, H. Ezura, K. Yamamoto, A. Hotta, T. Suzuki, Surf. Coat. Technol. 203 (2009) 1343.
[14] Y.D. Sun, J.Y. Yan, S. Zhang, F.Y. Xue, G.Q. Liu, D.J. Li, Vacuum 86 (2012) 949.
[15] Y.D. Sun, D.J. Li, C.K. Cao, N. Wang, J.Y. Yan, L. Dong, M. Cao, X.Y. Deng, H.Q. Gu, R.X. Wan, Surf. Coat. Technol. in press, (Available online May 31 2012).
[16] P.Y. Yashar, W.D. Sproul, Vacuum 55 (1999) 179.
[17] S. Veprek, S. Reiprich, Thin Solid Films 288 (1995) 64.
[18] X. Chu, M.S. Wong, W.D. Sproul, S.A. Barnett, J. Mater. Res. 14 (1999) 2500.
[19] B.L. Henke, J.Y. Uejio, H.T. Yamada, R.E. Tackaberry, Opt. Eng. 25 (1986) 937.
[20] D.J. Li, M. Tan, G.Q. Liu, M.Y. Liu, X.Y. Deng, H. Liu, X. Sun, Surf. Coat. Technol. 205 (2010) S5.
[21] S.P. Liu, Y.B. Kang, H. Wang, Q. Li, L. Dong, X.Y. Deng, D.J. Li, Mater. Lett. 62 (2008) 3536.
[22] B.M. Clemens, H. Kung, S.A. Barnett, MRS Bull. 24 (2) (1999) 20.
[23] L. Hultman, C. Engström, M. Odén, Surf. Coat. Technol. 227 (2000) 133.
[24] D.C. Kothari, A.N. Kale, Surf. Coat. Technol. 58–159 (2002) 174.
[25] K.W. Lee, Y.-H. Chen, Y.-W. Chung, L.M. Keer, Surf. Coat. Technol. 177–178 (2004) 591.